Photocatalysis

DOI: 10.1002/anie.201409906

Interface Engineering of a CoO_x/Ta_3N_5 Photocatalyst for Unprecedented Water Oxidation Performance under Visible-Light-Irradiation**

Shanshan Chen, Shuai Shen, Guiji Liu, Yu Qi, Fuxiang Zhang, and Can Li**

Abstract: *Cocatalysts have been extensively used to promote water oxidation efficiency in solar-to-chemical energy conversion, but the influence of interface compatibility between semiconductor and cocatalyst has been rarely addressed. Here we demonstrate a feasible strategy of interface wettability modification to enhance water oxidation efficiency of the state-of-the-art CoO_x/Ta_3N_5 system. When the hydrophobic feature of a Ta_3N_5 semiconductor was modulated to a hydrophilic one by in situ or ex situ surface coating with a magnesia nanolayer (2–5 nm), the interfacial contact between the hydrophilic CoO_x cocatalyst and the modified hydrophilic Ta_3N_5 semiconductor was greatly improved. Consequently, the visible-light-driven photocatalytic oxygen evolution rate of the resulting CoO_x/MgO(in)–Ta_3N_5 photocatalyst is ca. 23 times that of the pristine Ta_3N_5 sample, with a new record (11.3 %) of apparent quantum efficiency (AQE) under 500–600 nm illumination.*

Water oxidation is the crucial step in photocatalytic water splitting for renewable hydrogen production.[1] The efficiency of water oxidation is generally determined by three processes including light absorption, charge separation and transfer, and surface catalytic reactions.[2] To promote the water oxidation efficiency, loading of cocatalyst has become an important strategy.[3] Generally speaking, the structure of the cocatalyst is different from that of the semiconductor, so the formed interface between the semiconductor and cocatalyst should be rationally constructed to ensure an efficient charge transfer.[4] Previous efforts made on the cocatalyst have been predominantly focused on the development of cocatalyst species[5] and deposition methods,[6] but the role of the interface, especially its influence on the charge transfer and water oxidation efficiency has been rarely reported.

Besides the promotion of the charge separation and surface reaction, another key issue in improving the total water oxidation efficiency is to harvest a wide visible light range of sunlight.[7] Tantalum nitride (Ta_3N_5) has recently emerged as a promising particulate photocatalyst or photoanode for water splitting due to its wide range of visible light utilization (E_g: 2.1 eV) and suitable band edge position.[8] In addition, CoO_x was demonstrated to be an effective water oxidation cocatalyst for (oxy)nitride-based photocatalysts,[6] with which a high water oxidation efficiency (5.2 % at 500–600 nm) has been achieved for the Ta_3N_5 photocatalyst.[8b] However, from the viewpoint of hydrophilic–hydrophobic properties, an intimate interface between the hydrophobic Ta_3N_5 and hydrophilic CoO_x is not expected, which may render their interfacial charge transfer inefficient. Therefore, developing a strategy of interface engineering to improve the interfacial charge transfer of the CoO_x/Ta_3N_5 photocatalyst is highly desirable for a further promotion of its water oxidation efficiency.

In this work, an in situ or ex situ coating with a magnesia nanolayer was used to regulate the surface of Ta_3N_5 from hydrophobic to hydrophilic. The modified hydrophilic surface is found to be more favorable for an even deposition of hydrophilic CoO_x cocatalysts than the hydrophobic one, which is associated with a larger contact area, leading to a better interfacial charge transfer and water oxidation efficiency. In addition, the magnesia nanolayer also acts as a passivation layer to decrease surface defect sites of Ta_3N_5 and to inhibit the recombination of photoinduced carriers. With the optimized content of magnesia and CoO_x, we fabricated a highly efficient photocatalytic water oxidation system, whose AQE reaches 11.3 % at 500–600 nm, updating the world record of water oxidation efficiency on the particulate photocatalysts with an absorption edge at ca. 600 nm.

The magnesia modification on the surface of Ta_3N_5 was carried out by an "in situ" or "ex situ" method. For the "in situ" modification, typically, Ta_2O_5 powder was impregnated in the $MgSO_4$ aqueous solution and the dried mixture was then annealed in air at 1073 K for 2 h, forming a $MgTa_2O_6/Ta_2O_5$ mixture (Figure S1 in the Supporting Information). The oxide precursor was then nitrided under ammonia flow (250 mL min^{-1}) at 1223 K for 15 h, yielding MgO-modified Ta_3N_5 (denoted as MgO(in)–Ta_3N_5). Comparatively, the procedures for the "ex situ" magnesia modification are described as follows: 1) Ta_3N_5 was first synthesized by nitriding the Ta_2O_5 oxide at 1223 K for 15 h; 2) the prepared

[*] S. Chen, Dr. S. Shen, G. Liu, Y. Qi, Prof. F. Zhang, Prof. C. Li
State Key Laboratory of Catalysis, Dalian Institute of Chemical Physics, Chinese Academy of Sciences
Dalian National Laboratory for Clean Energy
457 Zhongshan Road, Dalian 116023 (China)
E-mail: fxzhang@dicp.ac.cn
canli@dicp.ac.cn
Homepage: http://www.canli.dicp.ac.cn
S. Chen, G. Liu, Y. Qi
University of Chinese Academy of Sciences
Beijing 100049 (China)

[**] We thank Prof. Kazunari Domen from the University of Tokyo for useful discussions. This work was financially supported by the Basic Research Program of China (973 Program: 2014CB239403); National Natural Science Foundation of China (No. 21361140346, 21373210). F. Zhang thanks the priority support from the "Hundred Talents Program" of the Chinese Academy of Sciences.

Supporting information for this article is available on the WWW under http://dx.doi.org/10.1002/anie.201409906.

Ta_3N_5 powder was impregnated in the $MgSO_4$ aqueous solution and then dried; 3) the mixture was nitrided under an ammonia flow (250 mL min^{-1}) at 1023 K for 1 h to convert $MgSO_4$ into MgO. The corresponding sample is denoted as MgO(ex)–Ta_3N_5. The formation of magnesia (MgO) was confirmed by XRD patterns (Figure S2) and HRTEM images, as discussed later. Here the content of the modifier is calculated on the basis of Mg element.

The surface hydrophilic–hydrophobic property of the modified and unmodified Ta_3N_5 photocatalysts was characterized by measuring the contact angle (CA), and the results were given in Figure 1. As expected, the pristine Ta_3N_5 sample

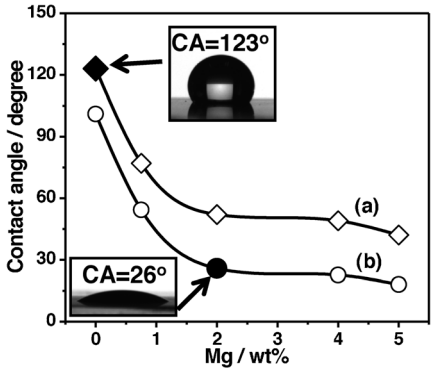

Figure 1. Contact angles (CAs) of a) MgO(in)–Ta_3N_5 and b) CoO_x/MgO(in)–Ta_3N_5 samples as a function of magnesium content. The content of CoO_x is 1 wt%; the inset figures are the stabilized water droplet pictures of samples: Ta_3N_5 (top); 1 wt% CoO_x/2 wt% MgO(in)–Ta_3N_5 (bottom).

shows a CA value of 123°, a typical surface hydrophobic feature. With increasing contents of magnesia modifier, the CA values gradually decrease until ca. 52° with a "saturated" magnesium content of 2 wt%. A similar CA value (50°) is also observed for the 2 wt% MgO(ex)–Ta_3N_5 sample. As for the CoO_x-deposited samples (Figure 1), the continuous decrease of the CA values with increasing the amount of magnesia also indicates the feasibility of magnesia modification in improving its surface hydrophilicity. It should be pointed out that CA values of the bare Ta_3N_5 films with or without light irradiation are not obviously changed (Figure S3).

The sample with in situ or ex situ magnesia modification exhibits a similar single phase of Ta_3N_5 in the XRD patterns (Figure S4), analogous particle size, and morphology in the SEM images (Figure S5) and close BET surface areas (ca. 9 $m^2 g^{-1}$), compared with those of the pristine Ta_3N_5. UV/Vis diffuse reflectance spectra (DRS) of all samples exhibit the characteristic absorption of Ta_3N_5 with an absorption edge at ca. 600 nm (Figure 2), but the absorption backgrounds originating from the formation of reduced tantalum species, e.g., Ta^{4+} ions, which commonly act as recombination centers of photogenerated carriers,[9] are decreased and increased, respectively, for the in situ and ex situ MgO-modified samples. The decrease of defect density caused by the in situ magnesia modification can be further confirmed by UV/Vis DRS (Figure S6) that the absorption backgrounds of the

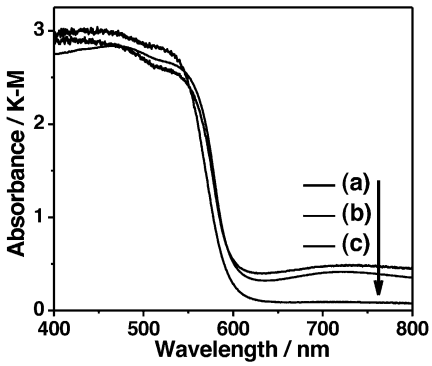

Figure 2. UV/Vis diffuse reflectance spectra of Ta_3N_5 based samples: a) 2 wt% MgO(ex)–Ta_3N_5, b) Ta_3N_5, c) 2 wt% MgO(in)–Ta_3N_5.

MgO-modified samples decrease with increasing magnesia content.

The decreased defect density of the MgO(in)–Ta_3N_5 sample may partially originate from magnesium ions doping according to the XPS spectra (Figure S7), in which the binding energies of Ta 4p, N 1s, and O 1s are shifted to lower regions after the magnesia modification, due to the smaller electronegativity of magnesium atoms compared to that of tantalum atoms. However, an unobvious change of peak positions is obtained in the XRD patterns (Figure S4), which is possibly due to the low concentration of doped magnesium ions and similar ion sizes of Ta^{5+} (78 pm) and Mg^{2+} (86 pm).[10] The magnesium ions doping into the crystal lattice of tantalum (oxy)nitride has also been proven by both experimental and theoretical results.[11] Based on the binding energies of 780.5 eV ($2p_{3/2}$) and 796.3 eV ($2p_{1/2}$) in the Co 2p XPS spectra (Figure S8), the deposited cobalt species are identified to be in the forms of both CoO and Co_3O_4[12] (denoted as CoO_x for simplicity).

As shown in Figure 3a, the deposited magnesium species are mainly loaded on the surface of Ta_3N_5 as a film with the thickness in the range of 2–5 nm. The formation of MgO was identified by a blank experiment in which pure $MgSO_4$ was treated with experimental procedures similar to steps 2 and 3 of the preparation of MgO(ex)–Ta_3N_5. According to the XRD patterns (Figure S2), a single phase of crystallized MgO can be confirmed for the as-obtained blank powder. It is worth noting that the formed MgO will be easily converted to $Mg(OH)_2$ once it is exposed to water.[13] This is confirmed by XRD patterns (Figure S2) and the HRTEM image (Figure 3c). Therefore, the successful modification of surface wettability is mainly ascribed to the formation of a MgO nanolayer, which can be converted to $Mg(OH)_2$ with plenty of surface hydroxy groups in the aqueous solution environment. As demonstrated by Figure 3b and d, the deposited cobalt cocatalysts on the surface of a magnesia-modified sample are mainly composed of CoO and Co_3O_4 oxides according to lattice spacing of the fringes (0.213 nm and 0.244 nm), in accordance with the Co 2p XPS results. As a comparison, the deposited CoO_x shows relatively decreased particle size and increased contact area on the magnesia-modified Ta_3N_5 sample (Figure 3d) compared to the pristine Ta_3N_5 sample (Figure S9). This is mainly ascribed to their remarkably

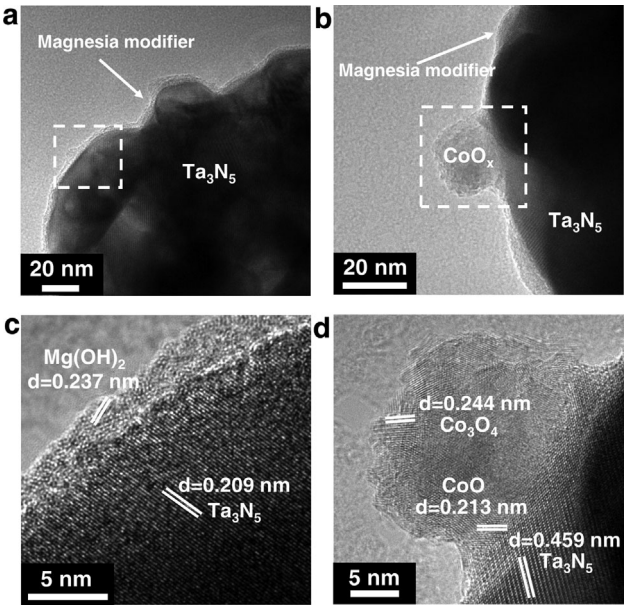

Figure 3. TEM and HRTEM images of a,c) 2 wt% MgO(in)–Ta_3N_5 and b,d) 1 wt% CoO_x/2 wt% MgO(in)–Ta_3N_5. The areas remarked by the rectangles (a, b) were correspondingly enlarged and shown in the HRTEM images (c, d).

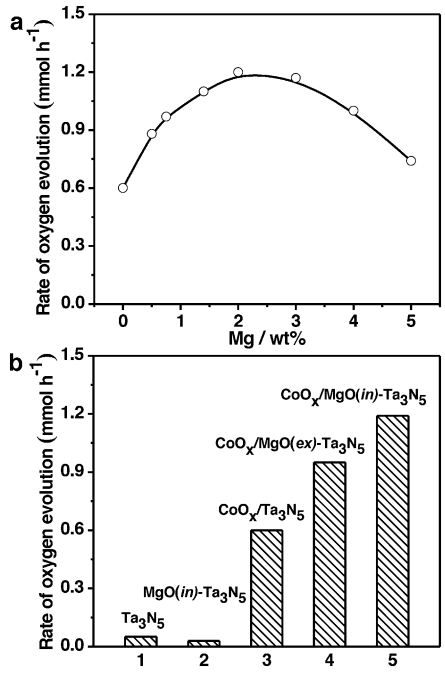

Figure 4. Rate of oxygen evolution on the Ta_3N_5-based photocatalysts: a) 1 wt% CoO_x/MgO(in)–Ta_3N_5 photocatalysts with different contents of magnesium. b) Typical Ta_3N_5-based photocatalysts (if it is contained, the content of magnesium or CoO_x is 2 wt% or 1 wt%, respectively). Reaction conditions: 0.15 g catalyst; 0.2 g La_2O_3 (as a buffer agent to maintain the pH value of the reaction solution to be ca. 8.5); 1.5 g $AgNO_3$; 150 mL H_2O; 300 W xenon lamp ($\lambda \geq 420$ nm); 0.5 h reaction time.

different surface wettability: the surface of magnesia-modified Ta_3N_5 is highly hydrophilic, whereas that of pure Ta_3N_5 is hydrophobic. To evenly deposit the hydrophilic CoO_x cocatalyst, the hydrophilic surface is more desirable.[14]

The photocatalytic water oxidation performance was evaluated using $AgNO_3$ as an electron acceptor under visible light irradiation ($\lambda \geq 420$ nm). No reaction occurs in the dark, and oxygen evolution begins with the onset of irradiation. A volcano-type curve of O_2 evolution rate depending on the CoO_x content is observed, and the maximum evolution rate of 0.6 mmol h^{-1} appears for the 1 wt% CoO_x/Ta_3N_5 sample (Figure S10). As shown in Figure 4a, the water oxidation activity is strongly dependent on the content of in situ magnesia modifier, and the optimal oxygen evolution rate (1.2 mmol h^{-1}) is achieved on the "hydrophilicity-saturated" sample with a magnesium content of 2 wt%. An excessive amount of magnesia modifier leads to a decrease of the water oxidation activity, which could be ascribed to the suppression of transfer of photoinduced carriers caused by the increased thickness of the MgO nanolayer.[15] The maximum O_2 evolution rate is ca. 23 times that of the pristine Ta_3N_5 sample. The possible promotion effect originating from SO_4^{2-} has been experimentally excluded. It is worth noting that the magnesia-modified Ta_3N_5 free of CoO_x deposition slightly deteriorates the performance of water oxidation, demonstrating the inert magnesia nanolayer itself is not active, and the photogenerated carriers need to tunnel through this layer for catalytic reactions.

Time courses of O_2 evolution on the 1 wt% CoO_x/2 wt% MgO(in)–Ta_3N_5 and 1 wt% CoO_x/Ta_3N_5 photocatalysts show that a much better photocatalytic activity and stability can be obtained on the sample with magnesia modification (Figure S11). Only a small amount of N_2 was detected in the initial stage of the reaction. Additionally, an HRTEM image (Figure S12) shows the well-maintained magnesia nanolayer on the sample after the reaction, which indicates the good stability of the modifier during the water oxidation process.

Figure 4b compares the O_2 evolution rates of some typical photocatalysts, and the order of catalytic activity is as follows: CoO_x/MgO(in)–Ta_3N_5 > CoO_x/MgO(ex)–Ta_3N_5 > CoO_x/Ta_3N_5 > Ta_3N_5 > MgO(in)–Ta_3N_5. For the optimal 1 wt% CoO_x/2 wt% MgO(in)–Ta_3N_5 sample, vigorous bubbles of O_2 can be observed under visible light irradiation (Supplementary Movie S1), and the AQE was measured (see Experimental Section) to be 11.3% at 500–600 nm, which is two times that of the state-of-the-art Ta_3N_5 photocatalyst modified with alkaline metal salts (5.2%).[8b]

As shown in Figure 5, the lifetime of photogenerated carriers on the CoO_x/Ta_3N_5 sample is obviously enhanced compared to that of the carriers on Ta_3N_5, manifesting the availability of CoO_x cocatalyst in inhibiting the recombination of photoinduced carriers.[6] Interestingly, a much stronger inhibition effect is observed for the samples of CoO_x/MgO(in)–Ta_3N_5 and CoO_x/MgO(ex)–Ta_3N_5 than that for the CoO_x/Ta_3N_5 sample. It should be pointed out that the magnesia modifier as an insulator is in essence unfavorable for the direct transfer of carriers. Therefore it is proposed that the enhanced lifetimes of carriers on the magnesia-modified samples should result from the interface effect between Ta_3N_5 and CoO_x, considering that the increased interfacial contact area (see HRTEM images of Figure 3d and Figure S9) is

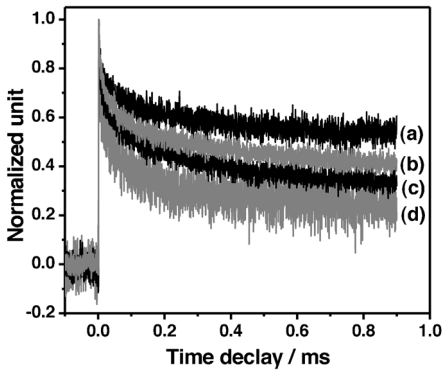

Figure 5. Decay of transient absorption of the representative Ta_3N_5-based photocatalysts in a vacuum: a) CoO_x/MgO(in)–Ta_3N_5, b) CoO_x/MgO(ex)–Ta_3N_5, c) CoO_x–Ta_3N_5, and d) Ta_3N_5. The pulse laser at 355 nm (1 Hz, 3 mJ/pulse) was used to excite the samples for the IR tests. In this figure, the contents of magnesium and CoO_x are 2 wt% and 1 wt%, respectively.

expected to provide more channels for the transfer of photoinduced carriers possibly through a tunneling effect.[16] The tunneling effect of electrons is actually confirmed by the HRTEM image (Figure S12), in which Ag nanoparticles photoreduced by the tunneled electrons, are found on the surface of the magnesia nanolayer. Similar tunneling effects were also reported in the literature.[15,17]

Compared with the 1 wt% CoO_x/2 wt% MgO(ex)–Ta_3N_5 photocatalyst, the 1 wt% CoO_x/2 wt% MgO(in)–Ta_3N_5 sample exhibits a relatively low defect density according to their UV/Vis DRS (Figure S13). In addition, both of them show similar surface wettability (CAs values: 26° in situ; 29° ex situ), crystallization (Figure S4), morphology (Figure S5), and surface area (ca. 9 $m^2 g^{-1}$). Therefore, their different amounts of defect sites might be responsible for their distinct charge separation efficiency and consequent water oxidation performance.

As a whole, the hydrophilic surface of the magnesia nanolayer is in favor of forming an even deposition of CoO_x cocatalyst leading to an enhanced interfacial contact area. On the other hand, partial doping of magnesium ions reduces the defect density of Ta_3N_5 during the magnesia modification. Both of these key roles (enhanced interfacial contact area and decreased defect density) contribute to the optimal charge separation and consequent water oxidation efficiency of the CoO_x/MgO(in)–Ta_3N_5 sample in this work. Additionally, the magnesia passivation layer may also protect Ta_3N_5 from being oxidized, thereby leading to an enhanced photocatalytic stability.[18]

In summary, we fabricated a hydrophilic CoO_x-modified Ta_3N_5 photocatalyst with an in situ-formed magnesia nanolayer on the surface for water oxidation under visible light irradiation. The corresponding AQE at 500–600 nm is 11.3%, which is two times that of state-of-the-art particulate photocatalysts with an absorption edge at ca. 600 nm. The essential roles of the hydrophilic interface modification with magnesia are proposed to enhance the interfacial contact area for the CoO_x/Ta_3N_5, and to decrease the defect density of the Ta_3N_5 semiconductor resulting from the passivation effect, both of which integrally promote the charge separation and consequent water oxidation efficiency. For the first time, we demonstrate the importance and feasibility of interfacial hydrophilic–hydrophobic compatibility between the semiconductor and cocatalyst in promoting water oxidation efficiency, and the interface engineering based on the hydrophilic–hydrophobic property is expected to be a general strategy for the design and fabrication of other highly efficient heterogeneous photocatalysts.

Experimental Section

Preparation of Ta_3N_5-based films for CAs measurements: Ta_3N_5-based films (2×3 cm^2) were prepared on FTO substrate by electrophoretic deposition using a potentiostat (ITECH IT6834). The CAs of water droplets for the prepared films were measured at ambient atmosphere using a CA analyzer (DSA100, Kruss GmbH, Germany).

Deposition of CoO_x: a calculated amount of cobalt nitrate was loaded on the Ta_3N_5 sample, then the as-impregnated powder was heated at 1023 K for 1 h under 250 mL min^{-1} NH_3 flow. The obtained sample was further calcined in air at 423 K for 1 h. Other detailed procedures can be found in the Supporting Information.

Received: October 9, 2014
Revised: December 14, 2014
Published online: January 21, 2015

Keywords: cocatalysts · interface engineering · photocatalysis · tantalum nitride · water splitting

[1] a) K. Maeda, K. Domen, *J. Phys. Chem. Lett.* **2010**, *1*, 2655–2661; b) J. S. Lee, *Catal. Surv. Asia* **2005**, *9*, 217–227; c) L. L. Duan, F. Bozoglian, S. Mandal, B. Stewart, T. Privalov, A. Llobet, L. C. Sun, *Nat. Chem.* **2012**, *4*, 418–423; d) A. Kudo, Y. Miseki, *Chem. Soc. Rev.* **2009**, *38*, 253–278; e) R. G. Li, F. X. Zhang, D. E. Wang, J. X. Yang, M. R. Li, J. Zhu, X. Zhou, H. X. Han, C. Li, *Nat. Commun.* **2013**, *4*, 1432.

[2] Y. Ma, X. L. Wang, Y. S. Jia, X. B. Chen, H. X. Han, C. Li, *Chem. Rev.* **2014**, *114*, 9987–10043.

[3] a) J. H. Yang, D. E. Wang, H. X. Han, C. Li, *Acc. Chem. Res.* **2013**, *46*, 1900–1909; b) D. E. Wang, R. G. Li, J. Zhu, J. Y. Shi, J. F. Han, X. Zong, C. Li, *J. Phys. Chem. C* **2012**, *116*, 5082–5089; c) B. J. Ma, F. Y. Wen, H. F. Jiang, J. H. Yang, P. L. Ying, C. Li, *Catal. Lett.* **2010**, *134*, 78–86.

[4] Z. Zhang, J. T. Yates, Jr., *Chem. Rev.* **2012**, *112*, 5520–5551.

[5] a) R. Abe, M. Higashi, K. Domen, *J. Am. Chem. Soc.* **2010**, *132*, 11828–11829; b) M. W. Kanan, D. G. Nocera, *Science* **2008**, *321*, 1072–1075; c) J. Sato, N. Saito, Y. Yamada, K. Maeda, T. Takata, J. N. Kondo, M. Hara, H. Kobayashi, K. Domen, Y. Inoue, *J. Am. Chem. Soc.* **2005**, *127*, 4150–4151.

[6] F. X. Zhang, A. Yamakata, K. Maeda, Y. Moriya, T. Takata, J. Kubota, K. Teshima, S. Oishi, K. Domen, *J. Am. Chem. Soc.* **2012**, *134*, 8348–8351.

[7] a) Y. Moriya, T. Takata, K. Domen, *Coord. Chem. Rev.* **2013**, *257*, 1957–1969; b) S. S. Chen, F. X. Zhang, *Chin. J. Catal.* **2014**, *35*, 1431–1432.

[8] a) G. Hitoki, A. Ishikawa, T. Takata, J. N. Kondo, M. Hara, K. Domen, *Chem. Lett.* **2002**, 736–737; b) S. S. K. Ma, T. Hisatomi, K. Maeda, Y. Moriya, K. Domen, *J. Am. Chem. Soc.* **2012**, *134*, 19993–19996; c) G. J. Liu, J. Y. Shi, F. X. Zhang, Z. Chen, J. F. Han, C. M. Ding, S. S. Chen, Z. L. Wang, H. X. Han, C. Li, *Angew. Chem. Int. Ed.* **2014**, *53*, 7295–7299; *Angew. Chem.* **2014**, *126*, 7423–7427.

[9] a) J. Q. Wang, S. Y. Su, B. Liu, M. H. Cao, C. W. Hu, *Chem. Commun.* **2013**, *49*, 7830 – 7832; b) Y. C. Lee, H. Teng, C. C. Hu, S. Y. Hu, *Electrochem. Solid-State Lett.* **2008**, *11*, P1 – P4.
[10] a) F. X. Zhang, K. Maeda, T. Takata, K. Domen, *J. Catal.* **2011**, *280*, 1 – 7.
[11] a) H. Schilling, M. Lerch, A. Börger, K. D. Becker, H. Wolff, R. Dronskowski, T. Bredow, M. Tovar, C. Baehtz, *J. Solid State Chem.* **2006**, *179*, 2416 – 2425; b) H. Wolff, M. Lerch, H. Schilling, C. Bähtz, R. Dronskowski, *J. Solid State Chem.* **2008**, *181*, 2684 – 2689.
[12] a) J. Jansson, A. E. C. Palmqvist, E. Fridell, M. Skoglundh, L. Österlund, P. Thormählen, V. Langer, *J. Catal.* **2002**, *211*, 387 – 397; b) M. P. Hyman, J. M. Vohs, *Surf. Sci.* **2011**, *605*, 383 – 389.
[13] J. T. Newberg, D. E. Starr, S. Yamamoto, S. Kaya, T. Kendelewicz, E. R. Mysak, S. Porsgaard, M. B. Salmeron, G. E. Brown, Jr., A. Nilsson, H. Bluhm, *Surf. Sci.* **2011**, *605*, 89 – 94.
[14] T. W. Kim, K. S. Choi, *Science* **2014**, *343*, 990 – 994.
[15] Y. W. Chen, J. D. Prange, S. Dühnen, Y. Park, M. Gunji, C. E. D. Chidsey, P. C. Mclntyre, *Nat. Mater.* **2011**, *10*, 539 – 544.
[16] H. F. Li, H. T. Yu, S. Chen, H. M. Zhao, Y. B. Zhang, X. Quan, *Dalton Trans.* **2014**, *43*, 2888 – 2894.
[17] a) P. P. Edwards, H. B. Gray, M. T. J. Lodge, R. J. P. Williams, *Angew. Chem. Int. Ed.* **2008**, *47*, 6758 – 6765; *Angew. Chem.* **2008**, *120*, 6860 – 6868; b) C. Prasittichai, J. R. Avila, O. K. Farha, J. T. Hupp, *J. Am. Chem. Soc.* **2013**, *135*, 16328 – 16331; c) K. Maeda, K. Teramura, D. L. Lu, N. Saito, Y. Inoue, K. Domen, *Angew. Chem. Int. Ed.* **2006**, *45*, 7806 – 7809; *Angew. Chem.* **2006**, *118*, 7970 – 7973; d) K. Maeda, K. Teramura, D. L. Lu, N. Saito, Y. Inoue, K. Domen, *J. Phys. Chem. C* **2007**, *111*, 7554 – 7560.
[18] K. Maeda, H. Terashima, K. Kase, M. Higashi, M. Tabata, K. Domen, *Bull. Chem. Soc. Jpn.* **2008**, *81*, 927 – 937.

